INTERMOUNTAIN POWER PROJECT

BURNER MODIFICATIONS

COMMENTS BY J.W. SMITH

SEPTEMBER 24, 1991

1. While the finite element analysis is simplified, it has helped to point out something that should be done in our new design.

   In either the original or new design there is a radial temperature gradient with the ID of the back plate hotter that the OD. If one just examines the radiation view angle along the radius of the back plate, this becomes apparent. The original design had the outside circumference of the back plate well shielded from furnace radiation, so this area would run near the windbox temperature while ID would run considerably hotter. With a flat ring and a radiant temperature gradient hotter on the inside than on the outside, the inside will be in compression tangentially while the outside will be in tension tangentially. For a linear temperature gradient, the stress values may be found by formula. With a non-linear gradient, the stress levels, assuming no buckling, may be found by a simple, linear finite element analysis as used by RJM.

   In any case, the significant stress levels shown are believable. With the high compressive stress on the inside, the inside will fail in a buckling mode with any number of failure shapes possible. It would take a very sophisticated non-linear program to predict buckling shape. Attached is an article from Mechanical Engineering discussing buckling prediction with such non-linear programs. The first mode of buckling might be a shape similar to a Belleville washer with higher modes of failure being a wavy shape along the ID. As suggested by RJM, this type of buckling failure would not be acceptable, as it would probably result in failure of the floating backing ring support clips.

   The idea of segmenting backing ring has merit as it addresses the buckling potential described above. B&W has used this design, for the same reason, for the refractory support ring of the CFB L-valves. The segments are essentially free plates, and if heated with a temperature gradient from one side to the other they, will deform with much lower stresses at the inner and outer fibers. Since in all scenarios it appears that the OD temperature will be less than the ID temperature, the various segments may touch at the OD. The gap between the segments would be set to taper from zero at the OD to 1/4" at the ID to accommodate the probable range of temperature gradient (see attached calculation).

Both the finite element analysis and the above discussion are simplistic. In fact, the heat flux and resulting temperature distribution are not uniform around the circumference of the plate. This non-uniformity will produce a number of other buckling potentials. Breaking the ring into segments is also useful for addressing non-uniformity as the segments are less restrained, and by their smaller size, are subject to less radial temperature gradients across their area.

The finite element analysis also has not considered another of the temperature gradients that contributes to the deformation of the back plate. There will be a temperature gradient through the thickness of the back plate (a 10,000 $B/ft^2/hr$ will result in a 35F Δ T). The furnace side of the back plate is heated by radiation from the furnace while the windbox side of the back plate is cooled by radiation to the windbox air (in addition to the convection cooling). The result is a heat flux and temperature gradient through the plate thickness. A ring (or circular disk) with a temperature gradient through it tends to deform like a Belleville washer (exactly as a regenerative air heater surface matrix bows as a result of the Δ T through the surface). The 10,000 $B/ft^2/hr$ heat flux (35 Δ T) will cause an axial displacement of 1/8" at the ID compared to OD (and both Δ T and displacement will be proportional to flux). This again would load the support clips on a ring. A segment also bows due to the gradient through the thickness, but here one can consider the edge clips to be restraints with the center surface bowing slightly towards the furnace as a result of the gradient. This process, again, reinforces the desirability of the segments.

2. The RJM concept of desirable swirl number of .8 on the inner zone and 0 on the outer zone is so distant from our experience that it is difficult to comment.

   The interesting task will be to assure that IPSC holds RJM responsible for the burner performance and for achieving an operating set up that produces proper flame stability, flame length, unburned carbon loss and NOx performance. IPSC should clarify that the RJM disclaimer on burner design does not apply to the operating performance and that RJM is responsible for proper burner operation. WE HAVE DONE THIS?

3. We have all stated to IPSC that recirculation is possible in an over swirl condition and have suggested to IPSC that they should reduce swirl on the present burners.

   I have yet to follow the rational in the recirculation parameter. Intuitively, I would think that, at the 0 vane angle on the inner air register, a stronger, no swirl inner air flow would have an improved

recirculation parameter. Comparing the curves of inner air flow, vane angle and outer register position to the curve of recirculation parameter, inner air vane angle and outer register position, the opposite trend is noted with a decrease in inner air flow providing a more positive recirculation parameter. This will be discussed with our CFD experts.

4. The RJM recommendation of 35/65 inner and outer split is within the range of operating parameters we would recommend. Our nominal sizing condition is more on the order of 25/75, but the actual operating parameters may well range to his recommendations.

   Balancing the outer area zones by shrouding is a nicety, but we would recommend that the balance be done with some outer zone swirl. If shrouds are installed to balance the burners with the registers wide open, then adding swirl to the outer zone (as will be required) will, to some degree, unbalance the burners.

5. The material thickness will remain as indicated on the B&W drawing. The increased thickness does provide added strength and resistance to buckling. Perhaps more significant, however, the increased thickness provides a greater flow area for heat conduction in the radial direction through the plate. This will help to minimize the radial temperature gradient and minimize component buckling. The material selection will be a mix of 304H and 309H since IPSC does not seem interested in the 800H and we have a hard time rationalizing the cost benefit relationship. Much of the material would 304H, but selected areas which are known to be the hottest spots will be made of 309H for its improved oxidation resistance. Parts to be made of 309H include the register doors and door stiffeners, the inner air sleeve, the throat sleeve, the coal pipe tip and the lighter shield. Material is being ordered on this basis.

6. With what RJM is recommending, flame scanning will be difficult. We would suggest that the burner observation door be used as the place to install the second flame scanner unless you believe that the observation port is definite need for burner set up.

Back Ring approx ~ 5'6 OD
~ 3'6 I.D

2'9" R
1'9" ±

Six Segments

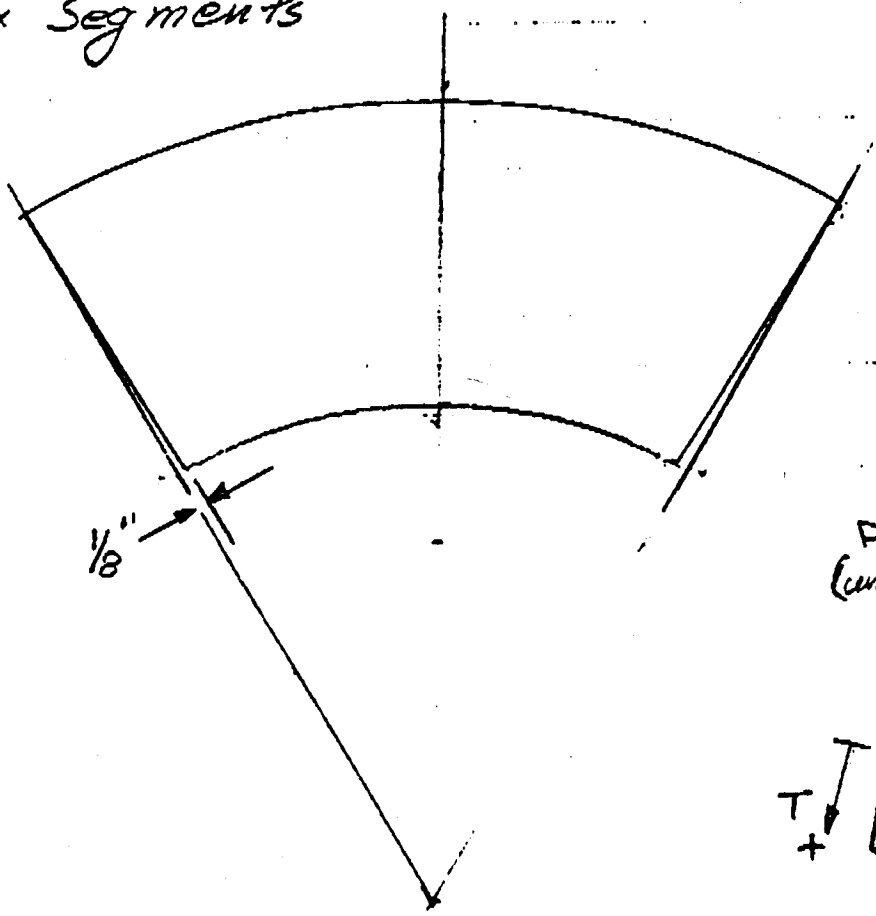

Rectangular Plate Analogy: (unrestrained plate)

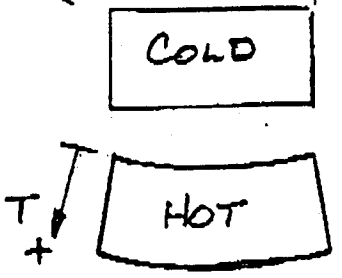

If the radial temperature gradient is constant, the dimensional changes should be uniform and the inside circumference growth, compared to the its size when at the temperature of the coldest circumference is approximately

$$\Delta l \approx \left(\frac{1}{6}\pi d\right) \alpha \Delta T$$

$d = 42"$ $\alpha \approx 10 \times 10^{-6}$

ΔT	Δl	
300	.066	2/32"
500	.110	7/64"
700	.154	5/32"
900	.198	7/32"

JW SMITH
9/18/91

Shop pins at 1/4" on ID & OD ~ 1/8" average

BEYOND BUCKLING

A NONLINEAR FE ANALYSIS

What happens to a structure after it collapses under compression? Nonlinear finite element analysis is becoming the engineer's equivalent of stop-action video.

DALE T. BERRY
DEVELOPMENT ENGINEER
MARC ANALYSIS RESEARCH CORPORATION
PALO ALTO, CALIFORNIA

For some time now, engineers have been using linear finite element analysis to determine the point of instability, or bifurcation, in buckling problems. Although linear methods often do a good job of estimating the load under which a structure buckles, they do not provide information about what happens after buckling. Neither can they account for potential nonlinearities that may have significant effects on the collapse load. In contrast, nonlinear analysis can now provide the means to follow the displacement history of a buckling structure up to the point of collapse and beyond.

The simulation of actual post-buckling behavior was recently demonstrated by Northrop Corporation and Marc Analysis Research Corporation. Northrop had been testing cylindrical aircraft panels to determine their behavior after they buckled under uniform longitudinal compression. These tests were designed to simulate conditions encountered in service, such as the compressive loading in the lower portion of the fuselage when an aircraft takes off, lands, or performs sudden airborne maneuvers.

The test panel was a stiffened composite cylindrical structure made of five to seven layers of woven graphite/epoxy cloth and unidirectional graphite/epoxy tape (Figure 1). It consisted of two L-section circumferential frames and three longitudinal stringers of hat-shaped section that reinforced its thin skin. These stringers were designed to provide the panel with load-carrying capacity even after the skin buckles.

The panel was loaded axially by prescribed edge displacements (Figure 2). Northrop was particularly interested in observing the panel's shape after the skin buckled, as the shape of the panel obviously affects its aerodynamic characteristics. The company asked Marc Analysis to study the buckling and post-buckling behavior of the panel using traditional linear and new nonlinear techniques. The results of these analyses could then be compared with Northrop's actual test results.

The analysts began by using Mentat, Marc's pre- and post-processor, to create a finite element model of the panel. The linear analysis was performed using standard techniques included in the Marc general-purpose FE code. Other portions of the same code were used to conduct the full nonlinear analysis.

LINEAR VERSUS NONLINEAR

A typical FE analysis consists of modeling a structure, and then determining how that model responds to applied loads. Linear methods assume that the behavior of the structure will not change as the applied load is increased. In other words, a structure's response to a load of 1000 pounds is assumed to be the same as 1000 times the structure's response to a load of one pound. This is the basic idea behind a linear buckling analysis, in which a small load is applied to a structural model and a buckling eigenvalue is extracted. The eigenvalue represents the number of times that the small load would have to be amplified in order to cause buckling.

Although linear buckling analyses are quite useful, they can miss some important phenomena. For instance, they do not take into account the changes in a structure's response as a load increases. The typical post-buckling curves of a perfect structure (Figure 3) show that the load-carrying capacity may drop sharply after buckling occurs, but that some residual strength remains. This is particularly true in axially loaded, stiffened cylinders and similar structures.

Real structures are never perfect. Imperfections, whether they are intentional or accidental, are always present. They start to influence the response at lower load levels than predicted for the perfect structure, and may cause the structure to buckle at a much lower load than calculated by a linear buckling analysis. In such cases, linear methods, which only provide an estimate of the buckling load, cannot be used to predict the behavior of the structure near bifurcation or the shape of the actual buckling mode. The linear buckling mode shapes often bear little resemblance to the actual buckled shape of the structure.

By contrast, nonlinear methods allow the behavior of the structure to change as the applied load changes. The current stressed state of the structure determines its response to additional loads. Nonlinear methods can also reveal the actual buckled shape, including the depth of the buckles.

In the past, nonlinear post-buckling analysis was considered difficult and expensive. Recent advances in computer hardware, however, have re-

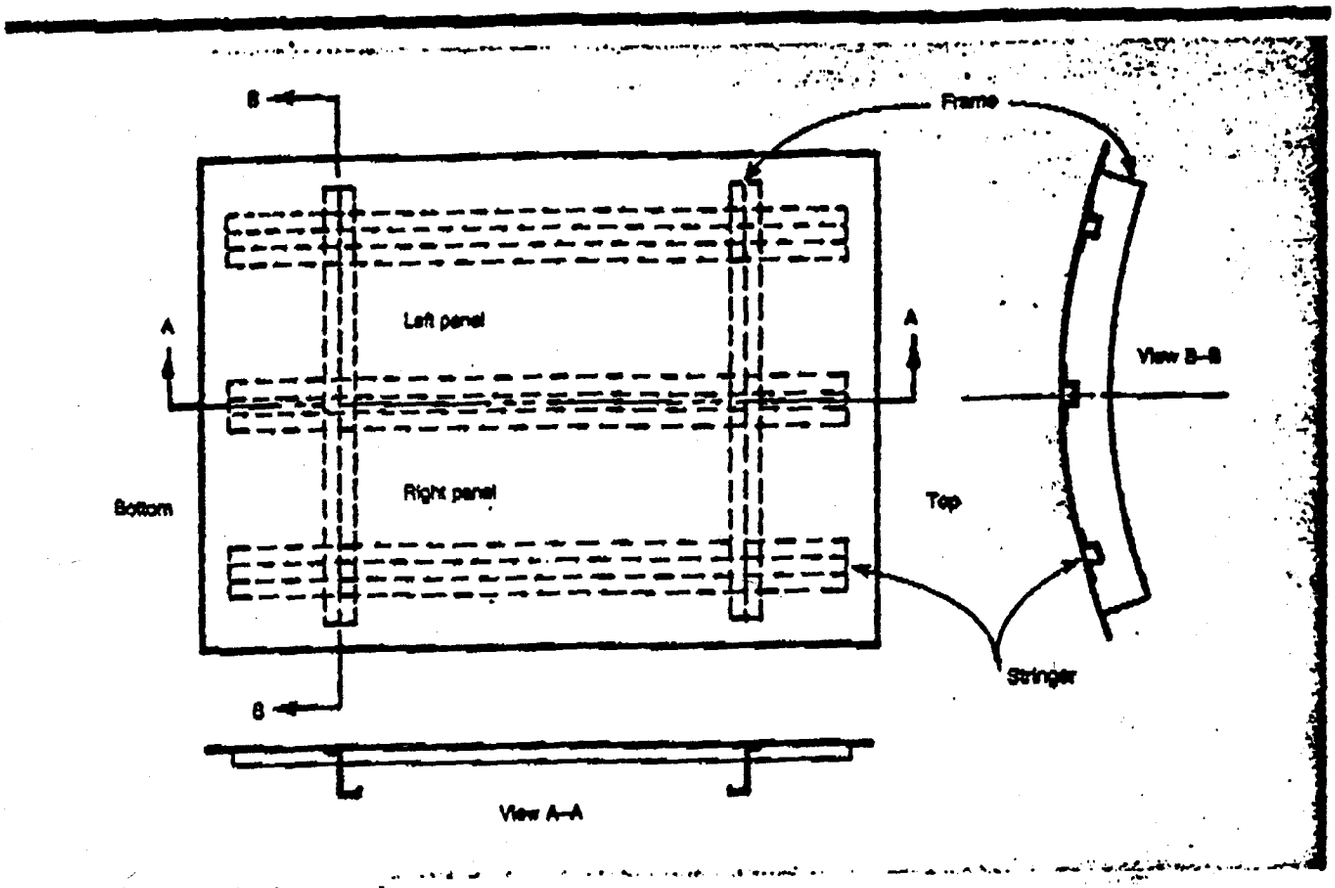

Figure 1. Composite fuselage panel.

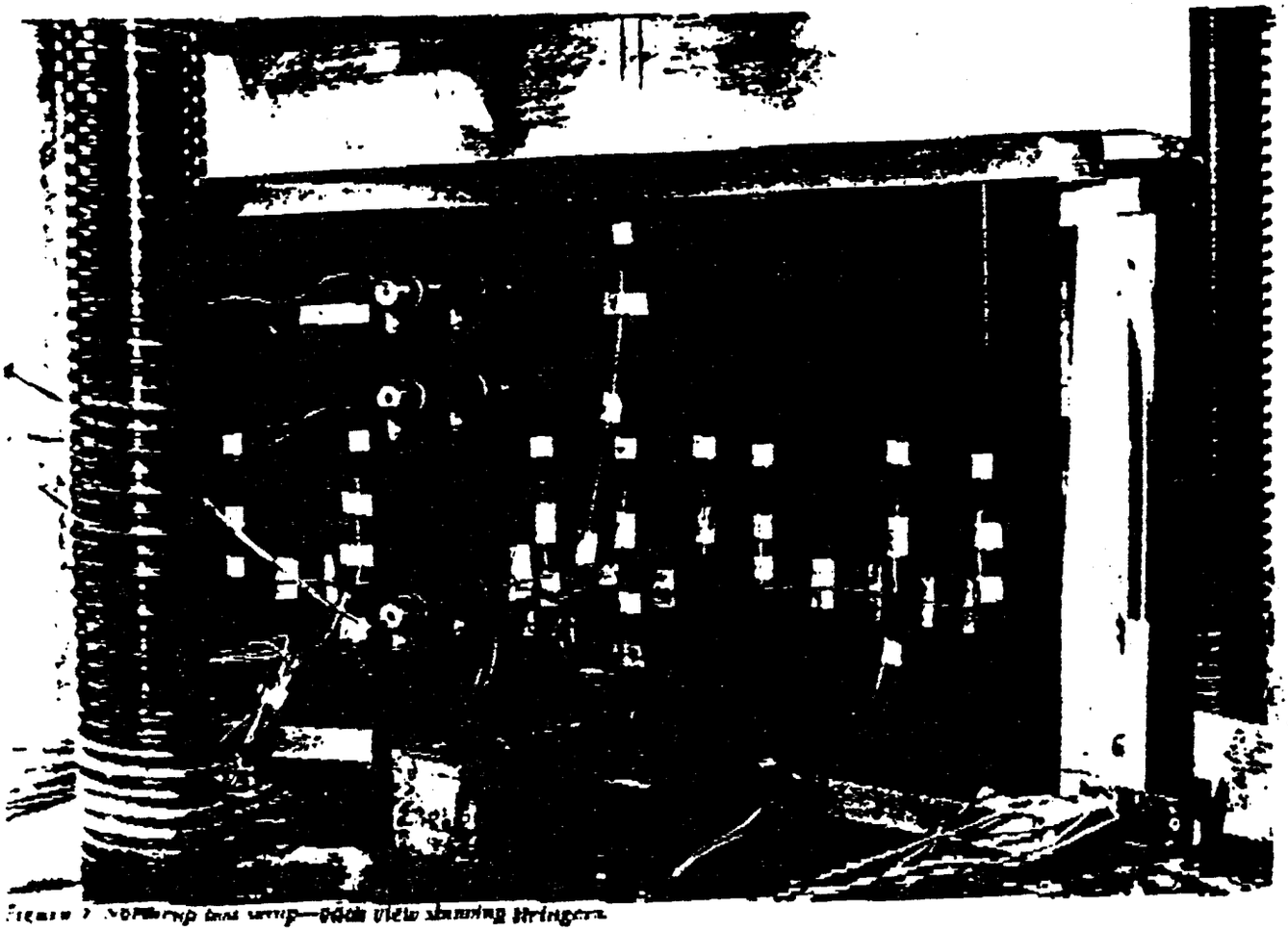

Figure 2. Pilgrim test setup—side view showing stringers.

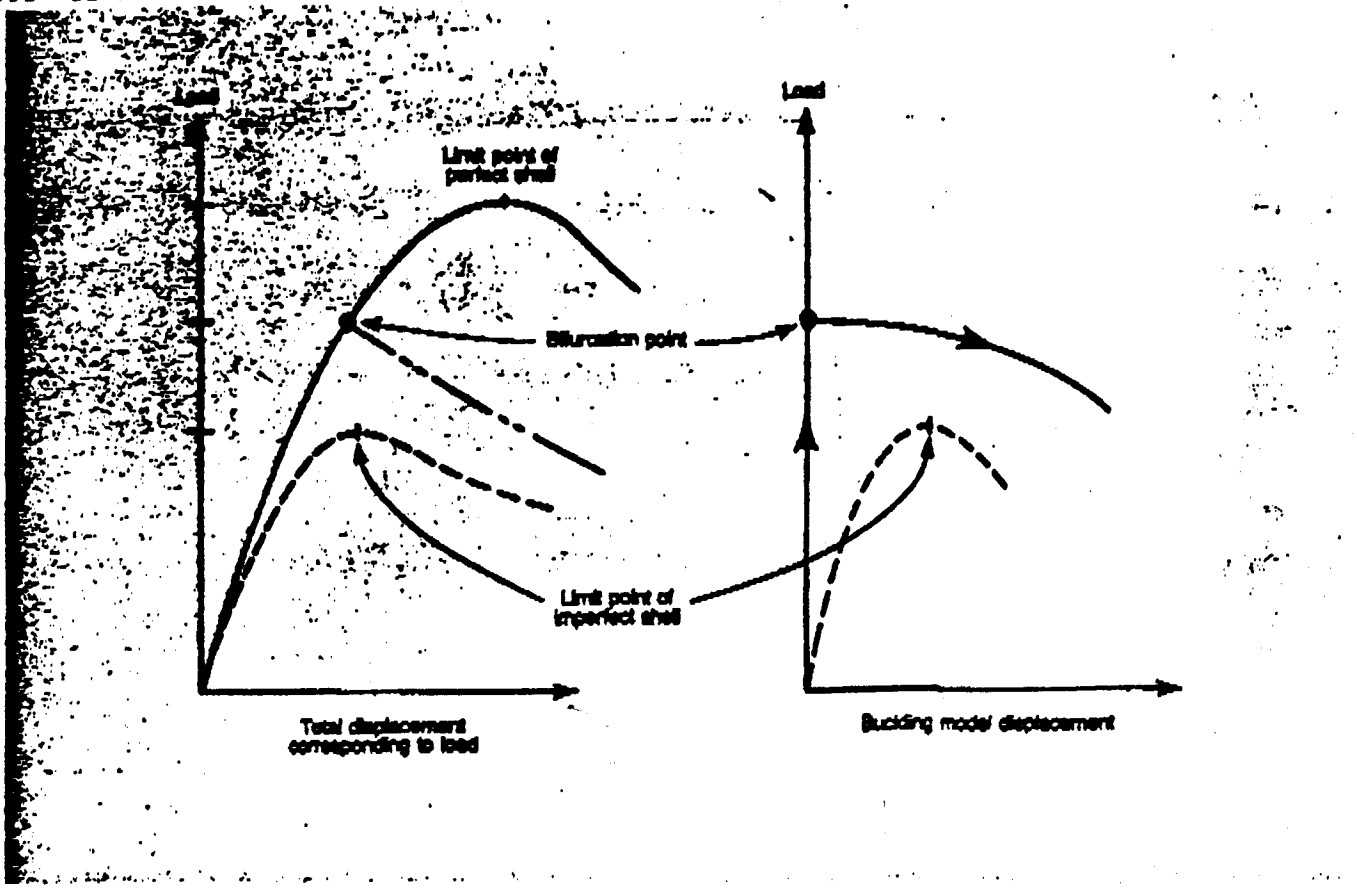

Figure 3. Typical post-buckling curves of perfect and imperfect structures.

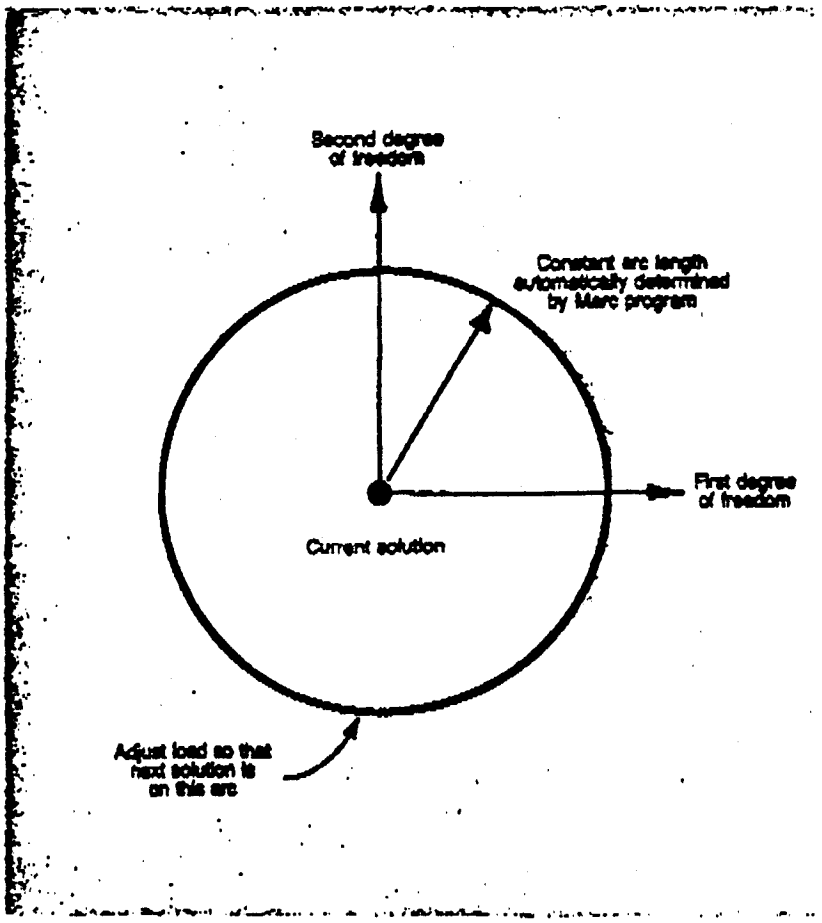

Figure 4. Limit on the change of position from one solution to the next.

duced the cost, and new interactive graphics packages are making nonlinear codes quite accessible. Also, new finite element algorithms bypass many of the computational difficulties inherent in post-buckling analyses.

One such algorithm that is particularly useful in buckling analysis is called the arc-length method. By adjusting the applied load on a structure, the algorithm holds constant a measure of the change in displacement within each increment. This constant value places a limit on the structure's unstable behavior (Figure 4). This adaptive algorithm is capable of automatically following the behavior of the structure through buckling and post-buckling phases.

COMPARISON OF ANALYTICAL AND EXPERIMENTAL FINDINGS

The finite element model of the panel, constructed with Mentat, uses an eight-node bilinear, layered thin-shell element chosen from the Marc element library (Figure 5). The stringers and frames were modeled using shell instead of beam elements because of the complex composite layups and because of the large size of the stiffeners in relation to the panel

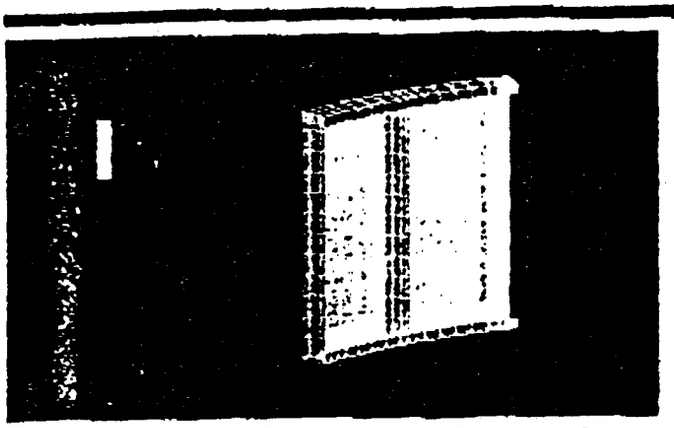

Figure 5. FE model for the linear and nonlinear analyses.

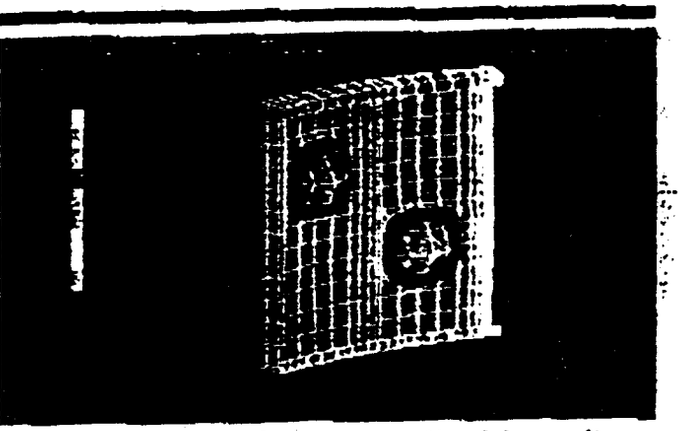

Figure 7. Buckling displacements predicted by nonlinear analysis after the first snap.

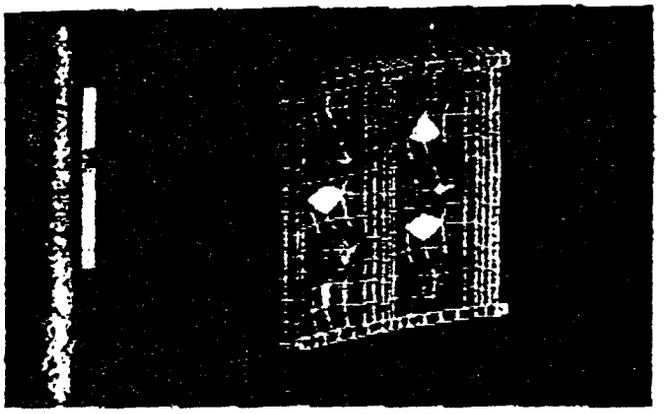

Figure 6. Buckling mode shape predicted by linear analysis.

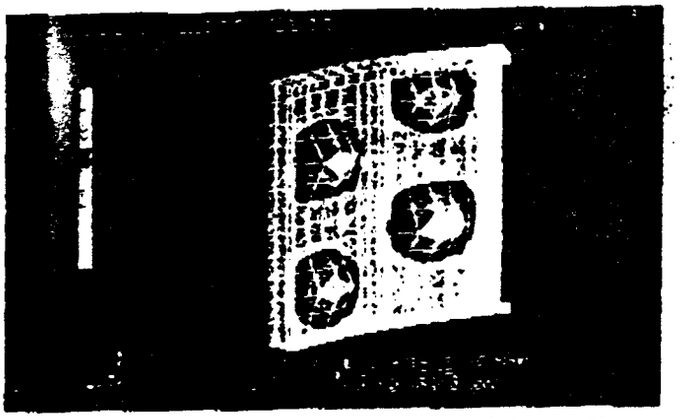

Figure 8. Buckling displacements predicted by nonlinear analysis after the second snap.

itself. In all, the model consisted of 414 shell elements and 34 truss elements for a total of 1256 nodes and approximately 2500 degrees of freedom. Each bay was a simple 12×4 mesh of shells.

A linear buckling analysis on the panel using standard eigenvalue procedures predicted the existence of a buckled shape with about five symmetrical half-waves in the axial direction (Figure 6). The buckling occurred at a stringer strain of .00055. Note that the linear analysis predicted that some of the buckling waves would project outward. This prediction conflicts with what is actually observed in cylindrical shell buckling—the crushing of a soft-drink can is an example.

In the nonlinear analysis, the goal was to compress the composite panel in a series of prescribed displacement steps, through at least one limit point, and on into the post-buckling range. Marc's automatic incrementing feature, which employs the constant-arc-length method, was used for this purpose. The analyst specified the initial step size (arc length), the desired number of iterations per increment, and the maximum step size allowed in any increment. The program's control option was used to specify the desired convergence criterion.

As the first steps were taken, at a displacement increment of 100 micro-inches per inch per step, the structure behaved linearly. After five increments, the maximum step size was decreased to 45 micro-inches per inch. As buckling occurred, the Marc program automatically adjusted the applied load to follow the changing load-carrying capacity of the structure.

The nonlinear analysis clearly demonstrated that the shape predicted by the linear buckling analysis never occurs in the actual panel. Instead, the panel first buckled into a two-bulge shape (Figure 7), which appeared at the end of increment 13 at a strain of 645 micro-inches per inch. The first sign of instability, however, occurred during increment 7, when the stringer strain increased from 545 to 590 micro-inches per inch. Both bulges in Figure 7 are inward, which indicates that interaction between the buckling modes caused asymmetric (inward) buckling. The results of this type of modal interaction can be seen only in nonlinear analysis; in linear analysis, each mode is assumed to be independent.

Because of the model's extreme instability near the buckling point, the program takes six increments to fully develop the buckled shape. The arc-length method prevents the solution from growing to the point that it causes the analysis to fail. The applied displacement changed very little during this transition phase, at the end of which the structure regained its stability.

As analysis increased the compressive load to nearly 1100 micro-inches per inch of stringer strain, a second snap-through to a four-bulge buckle occurred at increment 24, as shown in Figure 8. For the next ten increments, the four-bulge buckle grew steadily. The stringer strain increased from 1110 to 1540 micro-inches per inch, and the maximum normal deflection of the largest of these buckles grew from 0.22 inch to 0.26 inch. At this point, although structurally intact, the panel had already failed; the depth of the buckles would have degraded aerodynamic performance too severely.

As the nonlinear analysis continued, the structure assumed a three-

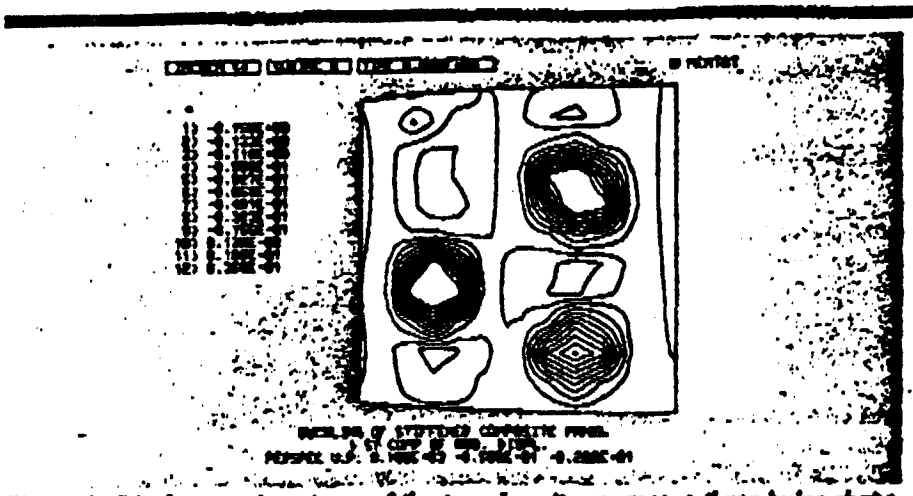

Figure 9. Displacement contours of the panel as it assumes a three-bulge shape during nonlinear analysis.

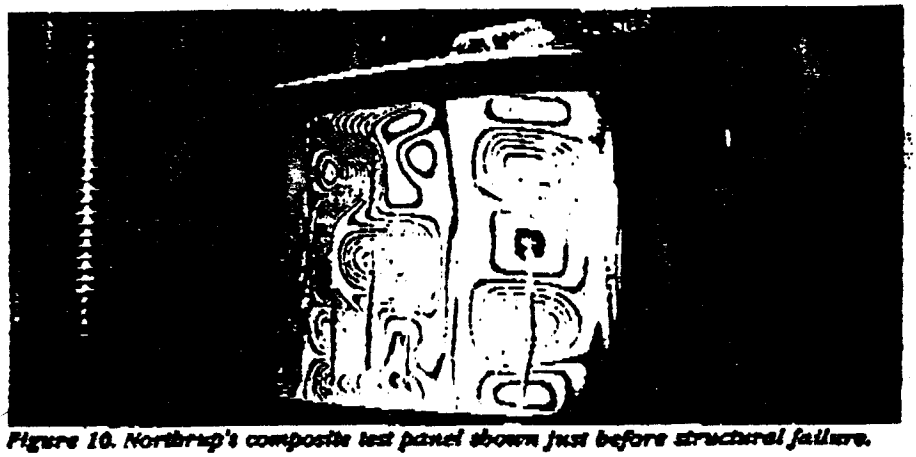

Figure 10. Northrop's composite test panel shown just before structural failure.

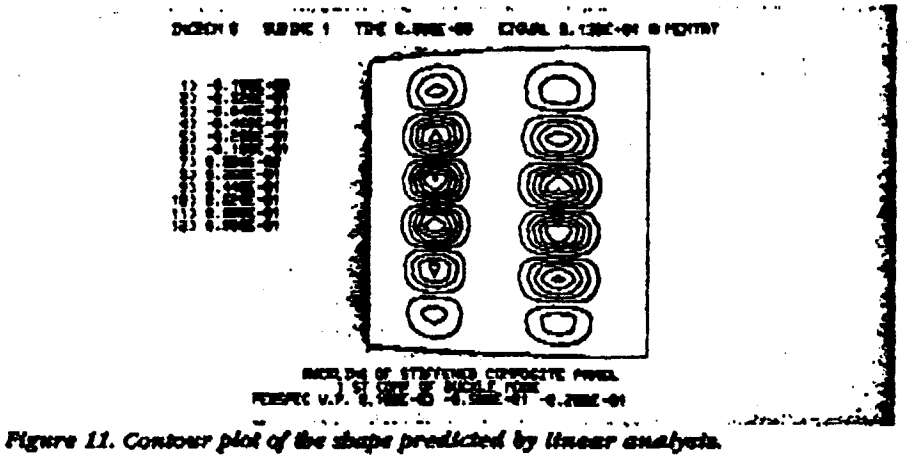

Figure 11. Contour plot of the shape predicted by linear analysis.

bulge shape. Displacement contours of this shape are shown in Figure 9, in which the two bulges in the left panel coalesced. These contours closely resemble those of the actual structure seen in Figure 10, which Northrop obtained by using a moiré fringe technique.

It should be noted that the results of the standard linear buckling analysis (Figure 11) are completely different from Northrop's experimental results. Comparing results from the linear analysis, nonlinear analysis, and actual test shows the validity of the nonlinear method in situations that are too complex for linear analysis.

Several figures generated by the nonlinear analysis further reveal the structure's behavior as it is subjected to increased compressive loads. Figure 12 is a plot of the total axial reaction force in the panel versus the axial displacement. Despite buckling of the skin, the slope of the load deflection curve changes very little. This indicates that most of the load is carried by the three unbuckled stringers.

The effects of the panel's snap-through on the localized load-carrying ability of the structure can be seen in Figure 13. The plot illustrates the behavior of the nodal reaction forces above the center of each panel as the axial displacement increases. For example, after the initial snap-through, the load-carrying capacity of the right panel decreases about 40 percent.

•

Nonlinear FE analysis can reduce the need for prototypes in the early stages of the design process. Nonlinear programs are becoming at once more sophisticated and easier to use. They can successfully simulate the behavior of a structure under stress—even after it has buckled. ■

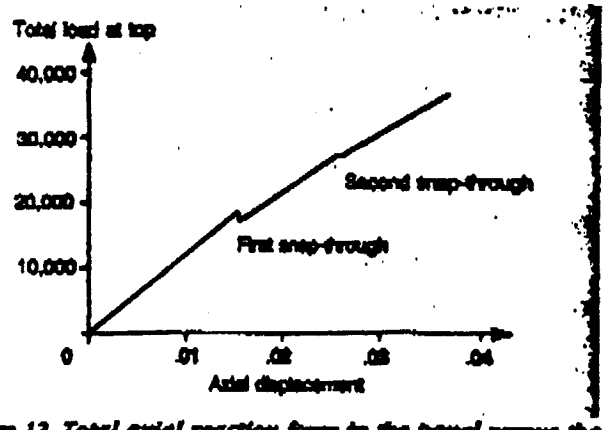

Figure 12. Total axial reaction force in the panel versus the axial displacement.

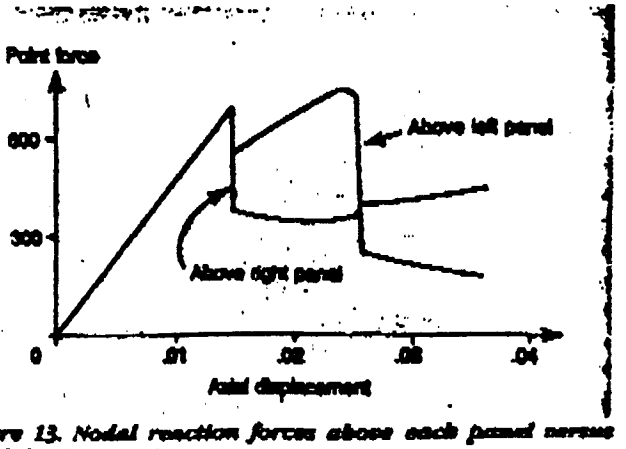

Figure 13. Nodal reaction forces above each panel versus axial displacement.